

SPACE DEMONSTRATION ANALYSIS RESULTS OF PHOTOCURABLE-SILSESQUIOXANE-COATED POLYIMIDE FILMS ONBOARD THE INTERNATIONAL SPACE STATION

Yugo Kimoto⁽¹⁾, Domestic International Standardization Committee for Atomic Oxygen Protective Coating Material for Spacecraft Applications

⁽¹⁾ Japan Aerospace Exploration Agency, 2-1-1 Sengen, Tsukuba, Ibaraki, Japan, kimoto.yugo@jaxa.jp

ABSTRACT

JAXA has developed the Exposed Experiment Handrail Attachment Mechanism (ExHAM), which is a general-purpose experimental platform on the International Space Station (ISS). ExHAM is mechanically attached on a handrail on some outer structure of the Kibo module (Japanese segment of the ISS), and provides new opportunities to conduct space exposure experiments on new materials, electrical components, and other subjects. Attachment operation by robotic arm is controlled by ground commands and requires no Extra Vehicular Activity (EVA) by the crew.

One ExHAM experiment involves the space durability testing of carbon nanotube (CNT). CNT without a coating may be damaged by atomic oxygen (AO). Therefore, photocurable-silsesquioxane-coated polyimide film is selected as protective coating material against AO. Three sets of CNT experimental trays on ExHAM were attached to the Kibo module, and then later retrieved on the ground.

This paper presents the analysis results of the three sets of retrieved photocurable-silsesquioxane-coated polyimide films. Measurement of the mass loss, thermal optical properties (i.e., solar absorptance, normal infrared emittance), and charging parameters (i.e., secondary electrons & photo emission coefficient, surface & volume resistivity) of the retrieved samples, and surface analysis by scanning electron microscope (SEM) were initiated. Cross-sectional micro observation by transmission electron microscope (TEM) was also done.

Space demonstration data were acquired from these analysis results, which indicate that photocurable-silsesquioxane-coated polyimide film has good durability in the space environment. Moreover, the second retrieved sample had a Micro Meteoroid Orbital Debris (MMOD) impact hole, measuring about 250 μm in diameter.

INTRODUCTION

The effects of the space environment on materials are very severe and complex, depending on the orbit in which the spacecraft is placed. Particularly in the orbit where the International Space Station (ISS) operates, interaction with both high-energy particles in space and the dominant neutral gas (AO) causes performance problems.

Space debris consisting of man-made objects orbiting around the Earth and no longer serving any useful purpose poses another hazard raising concern. Spacecraft surfaces are exposed to the full strength of solar UV radiation. In addition, surface degradation associated with contamination can adversely affect optical performance. The space environment and data on its effects are thus crucial for spacecraft design. In a space materials exposure experiment, the materials are exposed in space, retrieved on the ground and analysed, and thus the experiment samples provide an understanding of the actual space environment effects on materials. During its five years and nine months in Low Earth Orbit (LEO), NASA's Long Duration Exposure Facility (LDEF) provided information on the micrometeoroid or orbital debris environment based on impacts on its samples¹. The Material International Space Station Experiment (MISSE) series has been examined and exposed on the exterior of the ISS¹. ESA's Materials Exposure and Degradation Experiment (MEDET) on the ISS has also been implemented¹. The National Space Development Agency of Japan (NASDA), the forerunner of JAXA, implemented a space materials exposure experiment on the STS-85/Evaluation of Space Environment and Effects on Materials (ESEM) mission in 1997, and on the Exposed Facility Flyer Unit (EFFU) of the Space Flyer Unit (SFU) in 1996^{1,2}. The Micro-Particles Capturer (MPAC) and Space Environment Exposure Device (SEED) are the Japanese space materials exposure experiments on the ISS. MPAC is a micrometeoroid capture experiment, while SEED is a passive experiment designed to expose materials. There are two MPAC & SEED projects. One is for the Japanese Experiment Module Exposed Facility (JEM/EF) on the ISS, and the other is for the Service Module (SM) on the ISS¹⁻³.

JAXA developed a new materials exposure experiment system on the ISS. Taking advantage of JEM's unique function of having both an airlock and a robotic arm among modules on the ISS, the Exposed Experiment Handrail Attachment Mechanism (ExHAM) enables space experiments in an exposed environment by attaching it onto the JEM/EF⁴. ExHAM is a cuboid mechanism equipped with a grapple fixture on the upper surface for the robotic arm, with the Japanese Experiment Module Remote Manipulator System Small Fine Arm (JEMRMS SFA) grapple and attaching parts on the under surface for fixation to the handrail on the JEM/EF. Up to seven experiment samples can be loaded on the upper

surface, and with up to 13 samples on the side surfaces.

Several experiments have been in progress. Carbon nanotube (CNT) is considered a promising structural material in the aerospace industry, given its light weight and high strength compared with metal-based structural material. However, the degradation of CNT under exposure to the space environment is hardly known, and there are concerns about degradation due to AO, UV, radiation, thermal cycle, etc. Therefore, a Japanese research team conducted a CNT space exposure experiment using ExHAM⁵. AO is supposed to exert a strong oxidizing action on CNT, with such effects as generating defects in the bonding of carbon atoms, oxidation at the terminal end of carbon atoms, and a loss of carbon atoms as gas such as carbon dioxide.

Silsesquioxane (RSiO_{3/2}) has been researched as a potential AO protective-coating material for spacecraft applications⁶. The photocurable silsesquioxane “SQ series” offers a new type of organic–inorganic hybrid material that features photoinitiated polymerizable groups (organic units) introduced into silsesquioxane frameworks (inorganic units) as multifunctional groups at an intramolecular level. This coating has an excellent property for use as a space material coating. Therefore, this SQ-coated polyimide film is selected as protective coating material against AO.

This SQ coating solves such problems of conventional inorganic coatings as brittleness and low moisture resistance. Consequently, this SQ coating has advantages over conventional coatings. However, there is no document that specifies the requirements for coating characteristics, and an aerospace company typically selects and uses coatings based on internal experiments. Methods of testing and measuring each characteristic are not uniquely defined. A committee was organized in Japan to establish a method of evaluating various protection measures for coatings used in spacecraft, and clarify the effectiveness of AO protective coating technology. Table 1 lists the members of this committee (called the “domestic international standardization committee for atomic oxygen protective coating material for spacecraft applications”).

The committee's actual objective is to prepare an international standard draft that defines the general requirements for various coating characteristics, including those of existing coatings. Space demonstration data of the SQ-coated polyimide film retrieved from the ISS in the CNT project will be an appendix of this international standard.

Table 1. Member list (FY2017)

Status	Name	Affiliation
Chair member	Masahito Tagawa	Kobe Univ.
	Kazuhiro Toyoda	Kyushu Inst. of Technology
↑	Hiroshi Suzuki	TOAGOSEI
↑	Kazuaki Matsumoto	Tochigi Kaneka
↑	Ryo Yamashita	NEC
↑	Yutaka Kuribayashi	Mitsubishi Electric Corp.
↑	Naoki Yasuda	↑
↑	Yugo Kimoto	JAXA
↑	Naoko Baba	JAMSS
↑	Naomasa Furuta	TOAGOSEI
Associate member	Megumi Horiuchi	Ministry of Trade and Industry
↑	Yuki Shingai	↑
↑	Keita Yagi	↑
Secretariat	Yoichiro Uchida	SJAC

1. SPACE EXPOSURE EXPERIMENT ON ISS

As a CNT space exposure experiment, CNT twisted yarn and CNT epoxy composite material were selected as standard samples. As a comparative sample, a graphite sheet was chosen. SQ-coated polyimide film is selected as AO protective material for the CNT twisted yarn. The polyimide base film is APICAL-AH. Three sets of the SQ-coated polyimide are used for this CNT experiment. Table 2 shows the flight schedule. Figure 1 (a) shows the flight SQ-coated polyimide.

Table 2. Flight schedule of CNT on ExHAM

Sample ID	Position on ExHAM	Deployment	Retrieval	Exposed period [months]
#1	T(WAKE)	26 May 2015	13 June 2016	12
#2	R(WAKE)	26 May 2015	21 July 2017	26
#3	V(RAM)	11 Nov. 2015	13 Mar. 2017	16



(a) One of the CNT flight configurations on ExHAM



(b) *SQ*-coated polyimide

Fig. 1. Flight *SQ*-coated polyimide

2. ANALYSIS METHODS FOR RETRIEVED SAMPLES

Three sets of the *SQ*-coated polyimide are retrieved as well as CNT samples. Measurement of the mass loss, thermal optical properties (i.e., solar absorptance, normal infrared emittance), and charging parameters (i.e., secondary electrons & photo emission coefficient, surface & volume resistivity) of the retrieved samples, and surface analysis by SEM were initiated. Cross-sectional micro observation by TEM was also done.

3. ANALYSIS RESULTS AND DISCUSSION

3.1 Mass loss, thermal optical properties

Although there is no significant deterioration in the appearance of the three retrieved *SQ*-coated polyimides, there is a difference in colour between the non-space exposed surface and the exposed surface.

The mass reduction before and after flight was 1.373 mg (equivalent to 0.046 mg/cm^2) for sample T, 1.905 mg (equivalent to 0.064 mg/cm^2) for sample V, and 1.091 mg (equivalent to 0.036 mg/cm^2) for sample R with respect to the exposure area of about 30 cm^2 ($36 \text{ mm} \times 84 \text{ mm}$).

However, the influence of such handling as bending, tape fixing and cleaning is superimposed on the mass change of these samples. Mass reduction due to the penetration of Micrometeoroid and Orbital Debris (MMOD) is also superimposed in sample V as mentioned later.

We estimate AO fluence on ExHAM by using the NRLMSIS-00 model in the Space Environment & Effects System (SEES)⁷. We used the F10.7 and A_p index data available from the National Oceanic and Atmospheric Administration Space Weather Data and Products Database⁸ and do not consider flight-direction changes in our calculation. Table 3 shows the calculated results. The estimated value is on the Ram side, which is considered to be orders of magnitude smaller than that for samples T and R mounted on the Wake side. Thus, estimated AO fluence in these experiments is under the order of $1.34 \times 10^{21} \text{ [atoms/cm}^2\text{]}$. The fluence of AO ground irradiation is set as the target for this fluence.

Table 3. Estimated AO fluence by SEES

Position on ExHAM	Exposed period [months]	AO fluence [atoms/cm ²]
T(WAKE)	12	1.48×10^{21}
R(WAKE)	26	2.32×10^{21}
V(RAM)	16	1.34×10^{21}

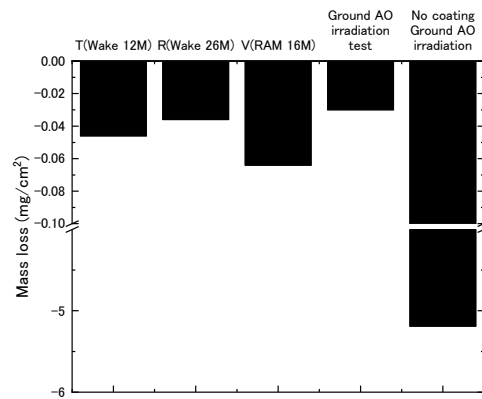


Fig. 2. Mass loss of the flight *SQ*-coated polyimide

Figure 2 plots all the data with the results of a ground AO irradiation test. The fluence of ground AO irradiation is $1.2 \times 10^{21} \text{ [atoms/cm}^2\text{]}$.

Although the mass measurement of the retrieved samples had a large error factor, the mass loss of the retrieved samples was at the same level as in the AO ground irradiation test. As the mass loss of the retrieved samples is almost one-hundredth of the no-coating sample in the ground AO irradiation test, excellent AO resistance is confirmed.

Figures 3 and 4 show changes in the solar absorptance and normal infrared emittance of three retrieved *SQ*-coated polyimides, respectively. The data of ground irradiated *SQ*-coated polyimide is also plotted. The

fluence of ground AO irradiation is 1.2×10^{21} [atoms/cm²]. Both solar absorptance and normal infrared emittance are largely unchanged. The results indicate that AO irradiation has a minor effect on the thermo-optical properties of the *SQ*-coated film.

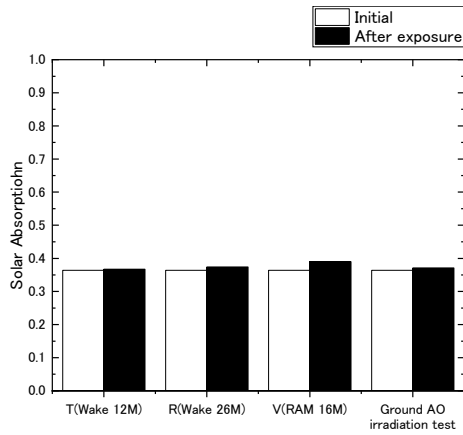


Fig. 3. Change in solar absorptance of the *SQ*-coated polyimide films

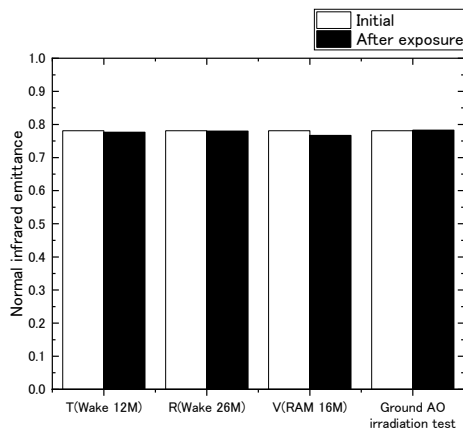


Fig. 4. Change in normal infrared emittance of the *SQ*-coated polyimide films

3.2 Surface analysis

The surface is observed by SEM. The surfaces of retrieved samples T and R were smooth, and no cedar-like shapes such as those of polyimide being attacked by AO were observed. Coating damage was observed in the scratched area. However, it is unknown when and how the scratches were made (e.g. before, during or after ground preparations, during crew operations in the ISS, in post ground transport). On the surface of retrieved sample V, cracks of several 10 to 100 μm in length were observed in the entire exposed part (Fig. 5). The enlarged SEM images of the cracked portion show that cracks occur with many foreign materials as the starting points, and that foreign materials are apparently present in the coating layer (Figs. 6 and 7). The surface without cracks is smooth, with no cedar-like shapes such as those of

polyimide being attacked by AO or any peeling of the coating being observed.

Such cracks are only found in sample V and were not observed in other exposed samples and on-ground AO irradiated samples.

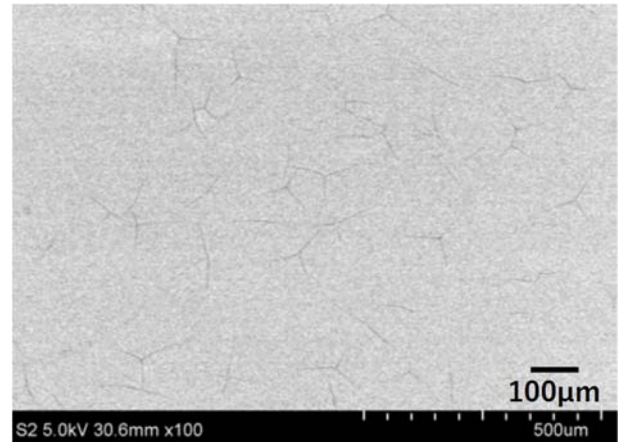


Fig. 5. SEM image of sample V

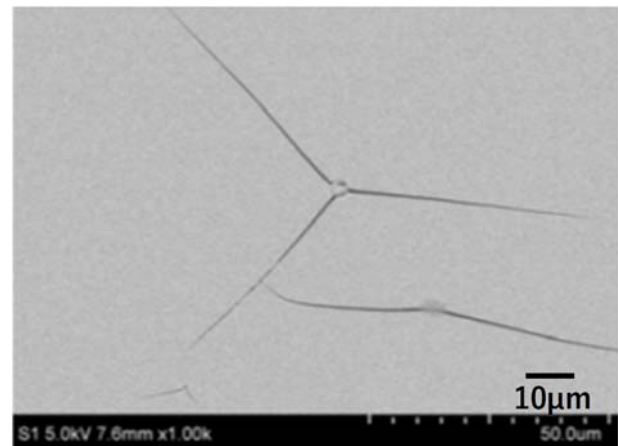


Fig. 6. SEM image of enlarged cracked portion on sample V

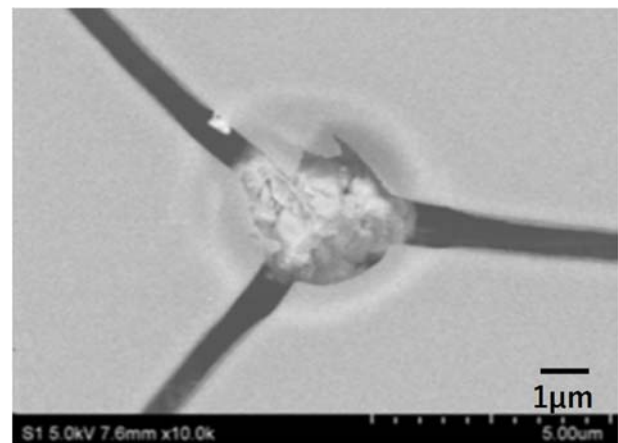


Fig. 7. SEM image of enlarged foreign material on sample V

Impact holes (through holes) due to MMOD are observed in two places in sample V. Near the impact hole of around 200 μm , cracks were observed in fine and high density (Fig. 8). The structure of the sample was destroyed, and its fragmented coating peeled off (Fig. 9).

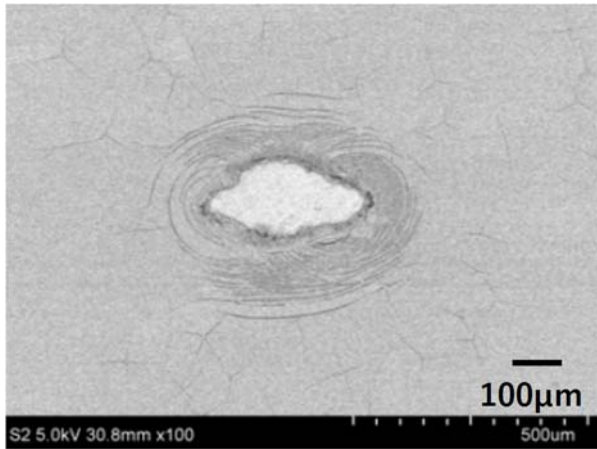


Fig. 8. SEM image of an impact hole due to MMOD on sample V

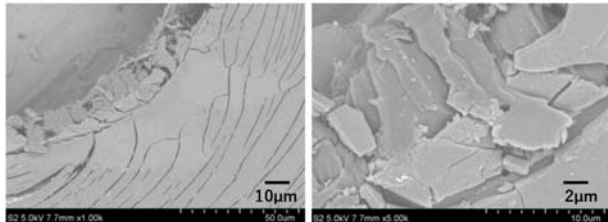
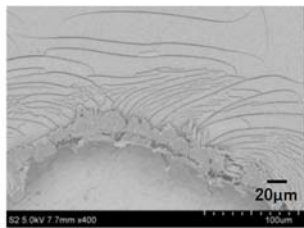


Fig. 9. SEM images of surface structures around an impact hole on sample V

The foreign materials in the crack observed in sample V measured about 2 to 5 μm in diameter, and many were covered halfway by the cracked coating. We found other foreign materials around the crack and analysed the components of the foreign materials. Figure 10 shows SEM images of the four foreign materials. These four foreign materials were analysed by Energy Dispersive X-ray spectrometry (EDX). Table 4 lists the EDX analysis results of the four foreign materials. Semi-quantitative analysis of foreign materials with EDX revealed that they contained Ca and P, which are not in the composition of the *SQ* coating itself. As Ca and P are components in the antiblocking (AB) agent of the base film, foreign material appears to be under the *SQ* coating, so foreign material in the crack could be AB agent.

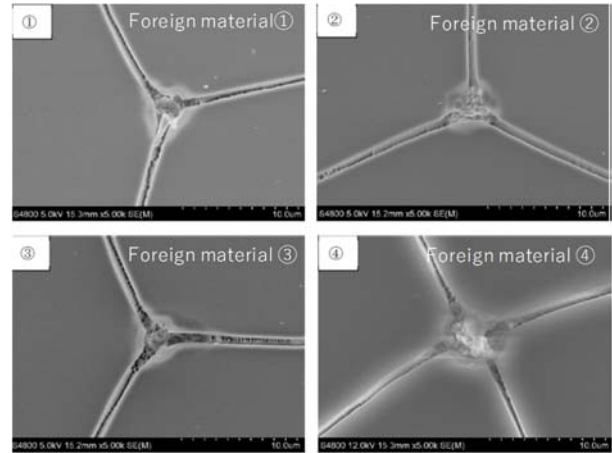


Fig. 10. SEM images of foreign materials in cracks on sample V

Table 4. Semi-quantitative analysis results by EDX

Foreign material	Atom components						Total (Atom%)
	C	O	Mg	Si	P	Ca	
①	7	39	*	*	14	40	100
②	4	47	0.1	0.9	13	36	100
③	11	26	0.2	0.7	14	49	100
④	10	26	N.D.	0.5	16	48	100
Smooth part	18	60	N.D.	22	N.D.	N.D.	100

* Although trace amounts of Mg- $K\alpha$ and Si- $K\alpha$ have been observed, calculations did not converge when Mg and Si were added. Therefore, Mg and Si are excluded from the calculation.

Cross-sectional micro observation by TEM is useful for confirming the formation of an oxide layer on the top surface. Contrast darkening was observed in the region of about 120 nm in the outermost layer of sample V (Fig. 11). The *SQ* layer was about 670 nm in thickness. Darkening of the contrast was also observed in the region of about 120 nm in the outermost layer.

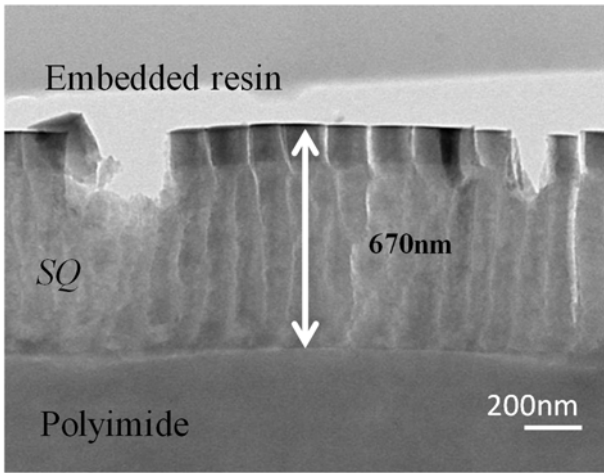
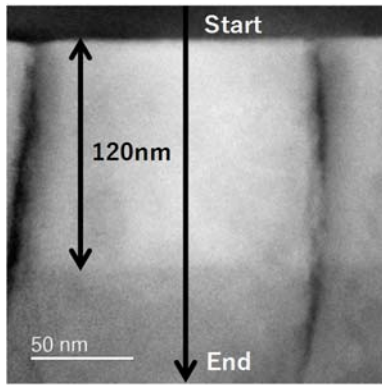
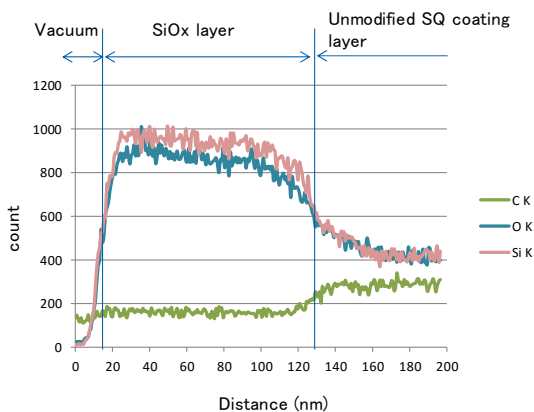


Fig. 11. TEM image of surface structure around an impact hole on sample V. Chippings or running cracks that occur vertically are those that occurred during the sample processing for TEM. Thus, these are artefacts not attributed to degradation by the space environment.



(a) Position of EDX line analysis



(b) EDX line analysis

Fig. 12. STEM/EDX analysis results

STEM/EDX line analysis of about 200 nm was performed from the surface layer to the lower layer in Fig. 11, where Si and O were mainly detected in the HAADF-STEM image where the contrast was observed to be brighter than the surroundings (Fig. 12). This region is

presumed to be a SiOx layer.

3.3 Charging parameters

Table 5 shows the measurement results of the charging characteristics. The space exposure samples T and V, and non-irradiated pristine SQ and SiOx coatings on APICAL-H films are measured for the charging characteristics. Regarding the secondary electron measurement, a pulsed electron beam was irradiated to the sample, and the current flowing to the sample and that flowing to the collector covering the sample were both measured. Here, -300 V and -250 V are applied to the sample and the collector, respectively. In addition, when the sample is an insulator, the measurement position is changed at every pulse of the electron beam⁹. For the photoelectron emission coefficient, vacuum ultraviolet rays were irradiated to the sample in pulses and the electron current emitted from the sample was measured. A wavelength selection filter was placed between the ultraviolet light source and the sample, and quantum efficiency was fitted from the photoelectron current curve obtained from each wavelength region.

The volume resistance and surface resistance were measured in a vacuum using the ASTM D-257 method¹⁰. A gold-coated circular electrode with a diameter of 16 mm was formed on the sample surface, and a gold-coated electrode with an inner diameter of 20 mm was formed on the outer side. The applied voltage is 500 V.

The secondary electron emission coefficient of sample V was almost equal to that of sample T, which was about 1.5 times larger than that of the pristine sample, which was close to SiOx. This is apparently due to SiO₂ being formed on the surface by AO irradiation. In contrast, the photoelectron current density of sample V (calculated from the photoelectron emission coefficient) was about double that of the pristine sample and about 1/4 of that of sample T on the wake side.

The volume resistance of sample V dropped to 1/10 of that of the pristine sample. This tendency is opposite to that of sample T where the volume resistance is increased by two orders of magnitude. As the secondary electron emission, photoelectron current density, and surface resistance of sample V are very close to the values of SiOx, it seems that SiO₂ is sufficiently formed on the surface by AO irradiation. It has also been clarified from past experimental results that applying irradiation with vacuum ultraviolet rays to SQ—the base material of samples T and V—increases the volume resistance. There is also the possibility that the volume resistance did not increase because vacuum ultraviolet rays are absorbed by SiOx formed on the surface of sample V.

Table 5. Charging characteristics

Sample	Secondary electron emission coefficient		Photoelectron current density [$\mu\text{A}/\text{m}^2 \text{ AM0}$]	Volume Resistance [$\times 10^{14} \Omega\text{m}$]	Surface resistance [$\Omega\Box$]
	dmax	E _{max}			
T(WAKE)	3.92	200	8.28	850	6.6×10^{15}
R(WAKE)	-	-	-	-	-
V(RAM)	3.70	400	1.9	0.9	1×10^{15}
Pristine SQ	2.4	300	0.9	9.0	$> 10^{16}$
Pristine SiOx	3.6	400	2.0	5.2	7.5×10^{13}

4. CONCLUSIONS

This paper presented the analysis results of three sets of retrieved photocurable-silsesquioxane-coated polyimide films. Sample V placed on the RAM surface showed the greatest variation in both mass loss and thermo-optic characteristics. However, as the mass loss of the retrieved samples is almost one-hundredth of the no-coating sample in the ground AO irradiation test, excellent AO resistance is confirmed.

There was a through hole on sample V that was attributed to a collision with MMOD, and near the through hole, many cracks originating from foreign materials were observed. It is unknown whether the cracks formed only in the SiOx layer or the exposed base polyimide after the SQ layer was cracked. As Ca and P were detected in the elemental analysis of foreign materials in the cracks, it is highly likely that these foreign materials are part of an antiblocking agent for the base film. According to TEM observation, the thickness of SQ decreased from 1 μm at the time of construction to about 670 nm. The thickness of SiOx formed on the outermost layer was about 120 nm. This layer is also analysed using the HAADF-STEM image, which shows that Si and O are mainly detected. The secondary electron emission coefficient of sample V was almost equal to that of sample T, and it increased about 1.5 times as compared with the pristine ground control sample. Conversely, the volume resistance of sample V decreased to 1/10 of that of the pristine ground control sample. This shows a trend opposite to that of sample T.

Based on these space environmental evaluation and demonstration data, proposals and discussions are currently in progress regarding “Atomic Oxygen Protective Coatings on Polyimide film” at the International Standardization Organization (ISO) / Technical Committee (TC) 20 / Sub Committee (SC) 14. These data will be an appendix of this standard.

ACKNOWLEDGEMENTS

This work is the result obtained by the “international standardization acceleration project (international standardization activity related to government strategy field) on atomic oxygen protective coating technology in the field of space material”. We appreciate the work of all persons involved in this project.

REFERENCES

1. D. L. Edwards, A. P. Tighe, M. V. Eesbeek, Y. Kimoto and K. K. de Groh, MRS BULLETIN, 35, 25, 2010.
2. Proc. International Symposium on “SM/MPAC & SEED Experiment”, JAXA-SP-08-015E, 2008.
3. Y. Kimoto, S. Ichikawa, E. Miyazaki, K. Matsumoto, J. Ishizawa, H. Shimamura, R. Yamanaka and M. Suzuki, Proc. of the 9th International Conference on “Protection of Materials and Structures from Space Environment”, p. 207, 2009.
4. T. Sato, H. Akagi, K. Matsumoto, “Overview and Future Plan of Exposed Experiment Handrail Attachment Mechanism (ExHAM)”, Aeronautical and Space Sciences Japan, 2018 Vol. 66, Issue 1, pp. 7-10, 2018.
5. Y. Fuchita, T. Hitomi, Y. Ishikawa, Y. Inoue, M. Karita, N. Baba, “Space Durability Test of Carbon Nanotube Part 3: Mechanical Properties of the Flight Specimens” (in Japanese), Proceedings of 61st Space Sciences and Technology Conference, JSASS-2017-4396, 2017.
6. Y. Kimoto, T. Fujita, N. Furuta, A. Kitamura, H. Suzuki, “Development of Space-Qualified Photocurable-Silsesquioxane-Coated Polyimide Films”, Journal of Spacecraft and Rockets, Vol. 53, pp. 1028-1034, 2016.
7. Space Environment & Effects System, <http://sees.tksc.jaxa.jp/>
8. Space Weather Data and Products, <https://www.swpc.noaa.gov/>
9. J. Wu, A. Miyahara, A. R. Khan, M. Iwata, K. Toyoda, M. Cho, X. Q. Zheng, “Effects of Energetic Electron and Proton Irradiation on Electron Emission Yield of Polyimide Induced by Electron and Photon”, Trans. JSASS Aerospace Tech. Japan, Vol. 12, No. ists29, pp. Pr_13-Pr_19, 2014.
10. ASTM D257, “Standard Test Methods for DC Resistance or Conductance of Insulating Materials”.